Robotica: (2020) volume 38, pp. 2023–2038. © Cambridge University Press 2020
doi:10.1017/S0263574719001796

New Robust Control Method Applied to the Locomotion of a 5-Link Biped Robot

Mohammad Mehdi Kakaei and Hassan Salarieh*

Department of Mechanical Engineering, Sharif University of Technology, Tehran, Iran
E-mail: mohammadmehdikakaei@gmail.com

(Accepted December 10, 2019. First published online: January 15, 2020)

SUMMARY
This paper proposes a new design of robust control combining feedback linearization, backstepping, and sliding mode control called FLBS applied to the locomotion of five-link biped robot. Due to the underactuated robot's model, the system has a hybrid nature, while the FLBS control can provide a stabilized walking movement even with the existence of large disturbances and uncertainties by implementing smooth chatter-free signals. Stability of the method is proven using the Lyapunov theorem based on the hybrid zero dynamics and Poincaré map. The simulations show the controller performance such as robustness and chatter-free response in the presence of uncertainty and disturbance.

KEYWORDS: Robust control; Stability; Hybrid nature; Underactuated; Biped robot; Locomotion.

1. Introduction

In the late 70s, movement of robots was in the form of quasi-static stable gate. This shape of movement was because of keeping the robot center of pressure remain strictly within the interior of the support polygon of their legs. Thus, it made them unable to walk fast, that is, the robot had a slow walking motion. Since early 80s, the research on dynamically stable movements began at the University of Tokyo, and later MIT developed them under the direction of Marc Raibert.[1,2] Because of the interest and importance of the robot passive movements, underactuated robots, having greater degrees of freedom compared to actuators setup on the robot, were developed. They require lower movement energy than fully actuated biped robots. Biped robots need to be investigated in many ways: energy, speed, versatility, robustness, etc. Regarding the dynamic movement, C. Chevallereau et al. introduced a control method assuming an instantaneous double-support phase (DSP) which can be applied to a five-link underactuated robot with one degree of underactuation. The reference path optimization was developed for five-link one degree of underactuation robot in their next work.[3,4] Grizzle et al. designed the first control method that analytically proves the stability of the three- and five-link robots with one degree of underactuation in rhythmic movement. In their modeling, the robot's movement was categorized into the single-support phase (SSP) and DSP. They created a concept of hybrid zero dynamic to stabilize the robot locomotion. In this concept for stabilizing robot, an appropriate time-invariant holonomic constraint was used. Moreover, it was attempted to converge the constraints to the zero value using feedback linearization control law. Finally, the control law was tested for the five-link underactuated robot (called RABBIT with point feet) and also the stability of system was studied using the Poincaré return map.[5–7] We used their five-link model and the concept of hybrid zero dynamics to control the robot in our work. In working with mechanical dynamics such as biped robots, the use of sensors injects some measurement noises in the control system. Measurement noises in addition to the system uncertainties and undesired external disturbances necessitate application of robust control methods. Tzafestas et al. in 1996 worked on the five-link

* Corresponding author. E-mail: salarieh@sharif.ir

https://doi.org/10.1017/S0263574719001796 Published online by Cambridge University Press

robot control using sliding mode method. The reference path was used to put constraints on the system. Their outcomes were also compared to the results achieved by the feedback linearization control method.[8] Lee et al. utilized the sliding mode method to control and stabilize the five-link robot and its combination with the neural network gets privilege to estimate the unknown model uncertainty of the biped robot system and nonlinear system parameters.[9] Moosavian et al. controlled a biped robot based on the zero moment point (ZMP) criterion to provide a stable motion for the biped robot. For this work, they utilized the sliding mode control approach and designed a new control method to reduce the chattering effects.[10] Nikkhah et al. applied the sliding mode controller to control the system with time-varying holonomic constraints related to the five-link underactuated robot with four actuators. They applied the external torque to the system in a short period of time to study the robustness against the disturbance.[11] Oza et al. studied a robust method to control the fully active seven-link robot using the reference inputs which is called second order sliding mode method.[12] Oviedo-Barriga et al. obtained a sliding mode controller based on a dynamic model using the conformal geometric algebra (CGA) approach.[13] Despite these works, finding a robust control law with chatter-free and smooth action is an important target in research. Chattering is a challenging issue in the controllers based on the sliding method, and some studies have been conducted to attenuate it.[14,15]

The main contribution of this study is the design of a robust chatter-free control law based on feedback linearization, backstepping, and sliding (FLBS) mode methods. It is applied to the locomotion of a five-link underactuated biped robot. The FLBS is formulated by three different approaches. To stabilize the locomotion of underactuated biped robot, the control method is combined with the concept of hybrid zero dynamics. In the control process, appropriate virtual constraints are applied to the system dynamics, thus the hybrid zero dynamic concept is considered to show a stable movement. To fulfill the mentioned constraints, feedback linearization approach is selected. Also to have a robustness property, it is combined with the sliding mode method. Finally, the backstepping control method as the third approach is combined with them and is utilized to provide a chatter-free controller. This form of combination creates a new method of control with a strong ability to resist against disturbances and chattering. The stability analysis of the closed loop system is performed using the Lyapunov stability theory and the Poincaré return map. A set of numerical simulations are presented to demonstrate the efficiency of the proposed controller through comparing with the sliding mode controller. Like,[8–13,16,17] it is common to use the sliding mode control in biped robots. Also, the simulations show that the proposed controller provides rapid convergence with small steady-state errors by providing low-amplitude control signals without chattering, and it can stabilize the system while large disturbances are applied.

The rest of the paper is organized as follows: The modeling of five-link underactuated biped robot is described in Section 2. In Section 3, the main theoretical contributions are presented, including a novel Lyapunov-based analysis for designing the controller. In Section 4, the robustness of the mentioned methods is shown by applying some parameter uncertainties and external disturbances to the system acting as a torque to the robot joints. Finally in the last section, some concluding remarks are presented.

Note: In this manuscript, all mathematical symbols other than the well-known sine, cosine, and saturation functions, are denoted, respectively, by sin, cos, and sat, and also the units of measurements, are written in *italic* fonts.

2. Modeling of the Robot

The locomotion is mostly in the sagittal plane. Thus, in this study this motion is analyzed in 2-D plane. In general, walking movement consists of successive phases; an SSP and the DSP. In each subdivision, equations with assumptions made for the five-link robot are obtained. Since the modeling was presented in refs. [2, 7], it is just briefly presented. The five-link biped robot includes one link for the trunk, and each leg has two links considering the knee (Fig. 1).

2.1. Dynamics of the robot during an SSP

This phase occurs when only one leg of the robot is on the ground. It is commonly assumed that no slip occurs between this leg and the ground.[5,7] Thus, the contact point acts as a pivot and the five-link model has 5 degrees of freedom. In this phase, the robot functions like an inverted pendulum. Actuators of the system, which apply joint torques, act as the external sources of energy. Four of them are located at the joints. Thus, the robot during an SSP is underactuated and has one degree of

https://doi.org/10.1017/S0263574719001796 Published online by Cambridge University Press

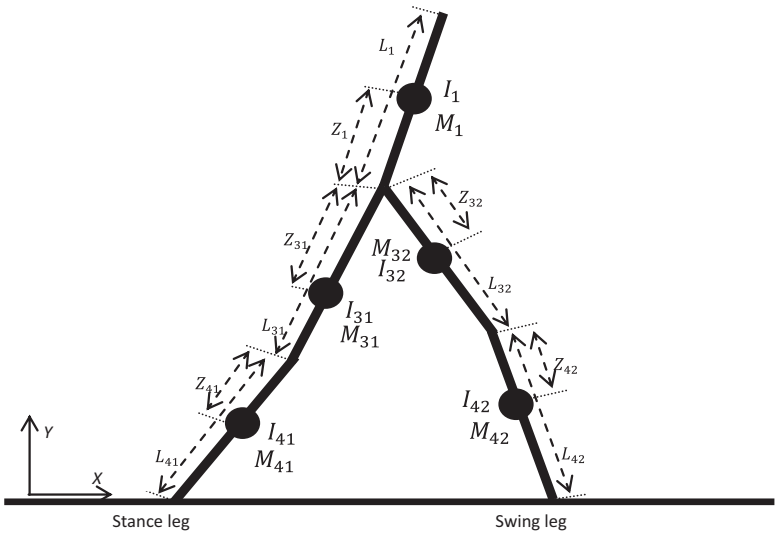


Fig. 1. The schematic of five-link underactuated biped Robot. The links of robot have mass and inertia and also in each joint an actuator is set. Thus, there are four actuators and the contact point between the stance leg and ground has no active moment (under actuation). For further use, the parameters of robot are given in Table I.

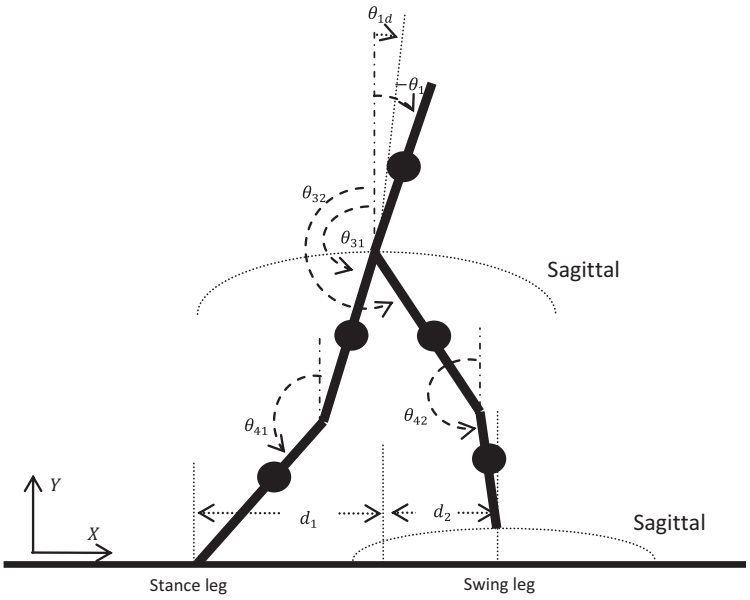


Fig. 2. The schematic of the aforementioned constraints on the considered model; angles are considered to be absolute. θ_{1d} is the desire angle that the trunk must have along the first constraint. d_1 and d_2 are the distances of hip from the end points of the stance leg and swing leg, respectively. The amounts of these parameters are given in Section 4.

underactuation. This is due to the fact that there is not any actuator between the end of stance leg and the ground. The absolute angles of links are the generalized coordinates of the system. In general using the Lagrange method, the dynamic equation of SSP is given by,

$$D\left(\theta_s\right)\ddot{\theta}_s + F\left(\dot{\theta}_s, \theta_s\right) + B.U = 0 \tag{1}$$

where D is the inertia matrix, the matrix F contains the Coriolis and gravitational effects, and B is the matrix that maps the actuator torques to the generalized forces. U is the actuator outputs and θ_s is the absolute link angles (see Fig. 2). The index (s) denotes SSP. More details on the governing Eq. (1) and also the D matrix and F, exist in the previous works such as refs. [2,5]. They are functions of the system parameters and coordinates, and for brevity we do not present them here.

https://doi.org/10.1017/S0263574719001796 Published online by Cambridge University Press

2.2. Dynamics of the robot in DSP

DSP occurs when the tip of the swing foot touches the ground. Also because of the consideration of instantaneous impact assumption in the time of this event, DSP is called the impact phase. We define impact surface (I) in the form of Eq. (2), which shows when the DSP happens.

$$I := \left\{ \left(\theta_s, \dot{\theta}_s\right) \in z \middle| \; Y_{end\ of\ swing\ leg} = 0 \; , \; X_{end\ of\ swing\ leg} \rangle 0 \right\} \tag{2}$$

The governing equations of this phase are obtained from the Lagrange method,

$$D_d(\theta_d)\ \ddot{\theta}_d + F_d\left(\theta_d, \dot{\theta}_d\right) = B_d.U + \delta F_{ext} \tag{3}$$

where θ_d denotes the orientation of the robot links in the space which depicts seven degrees of freedom (DOF). δF_{ext} is the other external generalized forces imposed to the system except the actuator torques in the joints. The index (d) denotes DSP. The impact is modeled as an instantaneous contact between two rigid bodies, because of the short contact time (it is a common assumption used in the literature[2,5,7,18–20]). Accordingly, the external forces in the impact phase can be shown as impulses. Also, it can be proven that the position states do not change, but it has a jump in the velocity states.[2,7] The other assumption is the absence of interaction between the stance leg with the ground exactly at the moment of impact.[2,7] As a result, using the mentioned simplifying assumption, differential equations will be converted to the following algebraic equations,

$$D_d(\theta_d)\ \left(\dot{\theta}_d^{+} - \dot{\theta}_d^{-}\right) = F_{ext} \tag{4}$$

where $F_{ext} := \int_{t^-}^{t^+} \delta F_{ext}\ (\alpha)\ d\alpha$, $\dot{\theta}_d^{+}$ is the velocity after the impact and $\dot{\theta}_d^{-}$ is the velocity before this event. The details of Eq. (3) and their parameters such as Dd are given in refs. [2,5].

Finally, these equations (Eqs. (1) and (4)) can be described in the state space, which is expressed as

$$\begin{aligned} \dot{z} &= f(z) + g(z)U \qquad z^- \notin I \\ z^+ &= \Delta\left(z^-\right) \qquad\quad z^- \in I \end{aligned} \tag{5}$$

where Δ is a mapping that transforms the states before the contact to the states after the contact. It should be pointed out that angular velocities before the contact are obtained via the previous SSP process.

2.3. Constraints

To stabilize the locomotion of biped robot using the concept of hybrid zero dynamics, the basic idea is to encode motion pattern in terms of a set of "posture conditions," which are briefly expressed as "constraints" on the position variables.[7] The constraints are defined on the robot movement to have a desired gate cycle. In addition, they cause the robot to have rhythmic movement. The number of constraints considered for this purpose should be according to the number of controllers used in the system. They are chosen for five-link robot as follows (see[7] for the further details).

1. Trunk will be at a certain angle.
2. Hip is always between the two legs.
3. Hip has a sagittal path.
4. End of swing leg has a sagittal path.

These constraints provide a simple shape of locomotion that the human can behave. They are shown in Fig. 2.

The controller should be designed such that the defined constraints are asymptotically stabilized. If these constraints are formulated as a vector function C, they make a surface (hyper-plane) with the following equation and properties (the Lie-derivative of the constraints with respect to f, $L_f C_i\ (\theta)$, is zero):

$$Z := \left\{ \left(\theta, \dot{\theta}\right) \in z \middle| \; C_i\ (\theta) = 0,\ L_f C_i\ (\theta) = 0\ , \quad i = 1:4 \right\} \tag{6}$$

https://doi.org/10.1017/S0263574719001796 Published online by Cambridge University Press

3. Control Design

As it was mentioned, the rhythmic movement includes a series of different phases that naturally repeat in every step. In our model, the five-link robot has two different phases. In every step, the dynamics change from SSP to DSP, and the impact between the end of swing leg and the ground causes the transition between these phases. In the concept of hybrid zero dynamics, the control method makes the mentioned constraints converge to zero before the impact occurs. In addition, the impact phase causes discontinuity in the system and imposes a new initial condition for the system applied to the next SSP, which provides a hybrid dynamics for the system. Here a robust control method is designed that can stabilize the underactuated five-link robot movement. In the nature, it has been seen that this type of underactuated system (such as human locomotion) has a stable and rhythmic movement as discussed in the literature.[2,5,7,21,22] Indeed there exists a limit cycle in these rhythmic motions, and the joints track their paths on that limit cycle after passing the transient time.[2,22–24] This limit cycle is produced by defining the desired constraints on the system of biped robot.[2,7,22,25] By using an acceptable control approach, the state trajectories are attracted by the mentioned limit cycle. In the literature, the Poincaré map method is commonly used for analyzing the stability of the limit cycles.[2,5,7,26] For using the Poincaré map analysis in this dynamics (locomotion), a surface that is transversal to the cycle should be defined, which is called the Poincaré section.[2] Usually, this surface is taken from the states at the impact time. The Poincaré map relates the first point of intersection to the Poincaré section with the next.[2] When the Poincaré section is defined as the surface I (Eq. (2)), the Poincaré map describes the function that relates the states of one impact to the states of the next impact. In order to have a stable and periodic cycle of locomotion, the successive points of Poincaré map should converge to a fix point which is indeed the desired limit cycle. In this case, the robot has a stable locomotion. In this approach, the stable periodic cycle is related to the stable equilibrium point of this function.[2] In summary, two necessary conditions are to be satisfied to create a Poincaré map. They are as follows:[2,11,22]

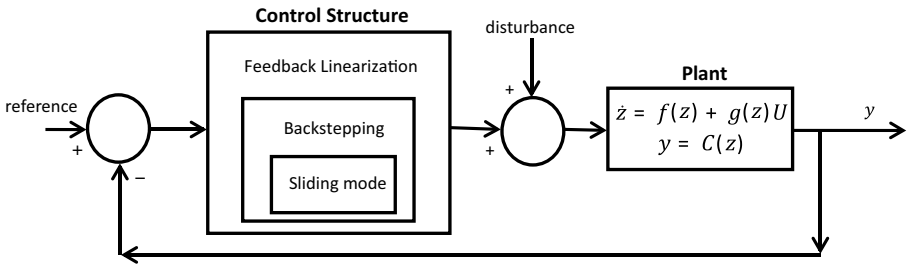
1. Describe the suitable constraint; $I \cap Z$ is a smooth manifold of states (I is the impact surface (Eq. (2)) and Z is the constraint surface (Eq. (6))) and second; the decoupling matrix $L_g L_f C(z)$ is invertible.
2. Design an appropriate control method that makes the constraints converge to the sliding surface in a finite time, and this surface should be asymptomatically stable.

The proof of satisfaction of the first condition is given previously in[2,7] for our five-link biped robot. Therefore, it is enough to show that the second condition is also satisfied. By showing these two conditions, there will exist a motion cycle. Finally by using the Poincaré method, it will be shown whether this rhythmic cycle is stable.

In this paper, the control method is proposed based on the combination of the sliding mode, the backstepping, and the feedback linearization methods. This goal is fulfilled by defining an asymptotically stable plane and trying to put the constraints' on this plane. It results in convergence of the constraints to zero and hence, a prerequisite for robot's locomotion is provided. The stability of the designed controller, named FLBS control method, is proven by using the Lyapunov method. It will be shown that the stability of the controlled system is exponential. To use the Lyapunov method, we try to find a positive definite function that is made of the states of the system variables. By showing the negative definiteness of the time derivative of this function, the asymptomatic stability of the designed control method can be proven. If the derivative of Lyapunov function is equal to or less than the Lyapunov function multiplied by a negative coefficient, then the exponential stability of the system is achieved.[27–29] Figure 3 briefly illustrates the FLBS control method in a simple block diagram. To summarize, in this approach at the first step, the feedback linearization method is utilized, thus some constraints, whose numbers are equal to the number of controllers, are defined in the system dynamics. Then robustness and chatter-free properties are added using the backstepping and sliding mode methods. By the backstepping method, new states based on the mentioned constraints are defined and in addition, the sliding mode surface is defined. The resultant is a first-order dynamic equation for the controller U that is from this process and also using the sliding reaching condition, the controller is obtained. Due to a special form of U-equation, the robustness and chatter-free behavior are guaranteed.

https://doi.org/10.1017/S0263574719001796 Published online by Cambridge University Press

(a)



(b)

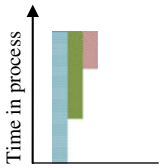
Time of application	Method	Important Notes
	Feedback Linearization	Define constraints
	Backstepping	Describe new state from constraints
	Sliding Mode	Define Sliding surface to guarantee asymptotic stability of constraints

Fig. 3. The structure of control approach; (a) a simple block diagram of the proposed approach, (b) important properties of each element in the proposed controller.

To design the FLBS control method, the following algorithm is traced. The constraints explained in Section 2.3 are considered as the output of the system,

$$y = C(z) \tag{7}$$

The general goal of controller is to stabilize the constraints. For this work, the error of the dynamics equation of the system can be obtained from Eq. (7). Since the constraints are holonomic and the actuator outputs are torques, the controllers in the feedback linearization method appear in the second time derivative of outputs and the relative degree of these equations is two. By using the standard Lie derivative notation,[2,30,31] direct calculation produces the following relations,

$$\frac{d}{dt}\begin{bmatrix} y \\ \dot{y} \end{bmatrix} = \begin{bmatrix} \dot{C} \\ L_f^2 C(z) \end{bmatrix} + \begin{bmatrix} 0 \\ L_g L_f C(z) \end{bmatrix} U \tag{8}$$

where

$$\dot{C} = L_f C(z) + L_g C(z) U \tag{9}$$

$$L_g C(z) = 0 \tag{10}$$

We will add two characteristics of robustness and chatter-free behavior to the controller. Two new state variables (Eq. (11)) are defined and the backstepping method is utilized.

$$\begin{cases} z_1 := y = C(z) \\ z_2 := \dot{y} - \alpha(z_1) = \dot{C} - \alpha(z_1) \end{cases} \tag{11}$$

Differentiating the variable z_1 with respect to time and substituting in the second variable (z_2), Eq. (12) is obtained.

$$\dot{z}_1 = z_2 + \alpha(z_1) \tag{12}$$

$\alpha(z_1)$ is a function of z_1 and it will be defined to remove existing nonlinear terms in the primary Lyapunov candidate (Eq. (13)) except multiplication of the first variable to the second.

$$V_1 := \frac{1}{2} z_1^2 \tag{13}$$

https://doi.org/10.1017/S0263574719001796 Published online by Cambridge University Press

To obtain $\alpha(z_1)$, the time derivative of V_1 is obtained,

$$\dot{V}_1 = z_1\dot{z}_1 = z_1\,(z_2 + \alpha(z_1)) \tag{14}$$

V_1 is a part of the general Lyapunov function that will be shaped in advance. Now $\alpha(z_1)$ is chosen as,

$$\alpha(z_1) \triangleq -\lambda_1 z_1 \tag{15}$$

By replacing it in the time derivative of V_1 (Eq. (13)), Eq. (16) is achieved.

$$\dot{V}_1 = -\lambda_1 z_1^2 + z_1 z_2 \tag{16}$$

where λ_1 is a positive value. Now the aforementioned process should be repeated. A new Lyapunov function that also have the second variable is written as (Eq. (17)), which is formed from the primary Lyapunov function V_1.

$$V_2 = V_1 + \frac{1}{2}z_2^2 \tag{17}$$

Differentiating V_2 with respect to time we have,

$$\dot{V}_2 = \dot{V}_1 + z_2\dot{z}_2 = -\lambda_1 z_1^2 + z_1 z_2 + z_2\dot{z}_2 \tag{18}$$

If the function (18) is negatively determined, then the constraints will converge to zero value. Of course, to have a negative definite function, the following sliding surface (S) is utilized, which makes the control method have more robustness.

$$S := \lambda_2 z_2 + \dot{z}_2 + z_1 \tag{19}$$

λ_2 is an arbitrary positive value. Based on Eq. (19), we have

$$\dot{z}_2 = S - \lambda_2 z_2 - z_1 \tag{20}$$

Substituting Eq. (20) in time derivative of the Lyapunov function (18), yields,

$$\dot{V}_2 = \dot{V}_1 + z_2\,(S - \lambda_2 z_2 - z_1) = -\lambda_1 z_1^2 - \lambda_2 z_2^2 + z_2 S \tag{21}$$

Now the surface S (Eq. (19)) is written in terms of the main variables of Eq. (7). By simplifying the sliding surface, we have,

$$\begin{aligned} S &= \lambda_2\left(\dot{C}(z) + \lambda_1 C(z)\right) + \left(\ddot{C}(z) + \lambda_1\dot{C}(z)\right) + C(z) \\ &= \lambda_2\left(L_f C(z) + \lambda_1 C(z)\right) + \left(L_f^2 C(z) + L_g L_f C(z)U + \lambda_1 L_f C(z)\right) + C(z) \end{aligned} \tag{22}$$

Differentiating S with respect to time yields,

$$\begin{aligned} \dot{S} &= \lambda_2\left(L_f^2 C(z) + L_g L_f C(z)U + \lambda_1 L_f C(z)\right) + L_f C(z) + L_g L_f C(z)\dot{U} \\ &+ \tfrac{d}{dt}L_f^2 C(z) + \tfrac{d}{dt}L_g L_f C(z)U + \lambda_1\left(L_f^2 C(z) + L_g L_f C(z)U\right) \end{aligned} \tag{23}$$

Now the general Lyapunov (Eq. (24)) including S, z_2, and z_1 variables is formed as,

$$V := V_2 + \frac{1}{2}S^2 \tag{24}$$

Differentiating V with respect to time results in,

$$\dot{V} = \dot{V}_2 + S\dot{S} = -\lambda_1 z_1^2 - \lambda_2 z_2^2 + S\left(\dot{S} + z_2\right) \tag{25}$$

If this derivative is negative definite, the origin in the error dynamics is asymptotically stable. To this end, the last term of Eq. (25) is set as,

$$\left(\dot{S} + z_2\right) := -k\,\mathrm{sign}\,(S) - \lambda_3 S \tag{26}$$

https://doi.org/10.1017/S0263574719001796 Published online by Cambridge University Press

where λ_3 and k are arbitrary positive values. Substituting Eq. (8) into Eq. (26) results in,

$$\begin{aligned}\lambda_2\left(L_f^2C(z)+L_gL_fC(z)U\ +\lambda_1L_fC(z)\right)+\lambda_1\left(L_f^2C(z)+L_gL_fC(z)U\right)+\tfrac{d}{dt}L_f^2C(z)\\ +\tfrac{d}{dt}L_gL_fC(z)U+L_gL_fC(z)\dot{U}+2L_fC(z)+\lambda_1C(z)=-k\text{sign}\,(S)-\lambda_3S\end{aligned}\tag{27}$$

Eq. (28) is demonstrated as a dynamics for U in order to provide negative derivative for the Lyapunov function of Eq. (24). From Eq. (27), the control signal should satisfy the following equation,

$$\begin{aligned}\dot{U}=-L_gL_fC(z)^{-1}(k\text{sign}\,(S)+\lambda_3S+L_f^2C(z)+\lambda_1\left(L_f^2C(z)+L_gL_fC(z)U\right)\\ +L_gL_fC(z)U+\lambda_2\left(L_f^2C(z)+L_gL_fC(z)U+\lambda_1\dot{C}(z)\right)+2\dot{C}(z)+\lambda_1C(z)\end{aligned}\tag{28}$$

Finally, the Lyapunov function and its derivative are rewritten as,

$$V=\frac{1}{2}z_1^2+\frac{1}{2}z_2^2+\frac{1}{2}S^2\tag{29}$$

$$\dot{V}=-\lambda_1z_1^2-\lambda_2z_2^2-\lambda_3S^2-kS\text{sign}\,(S)=-k_pV-k\,|S|\tag{30}$$

The derivative of the Lyapunov function is always a negative definite. Based on Eq. (30), the origin of the error dynamics is globally exponentially stable. The $k\,|S|$ term causes that the error dynamics to reach a sliding surface in a finite time and converge to zero value on this surface. Of course, by increasing the coefficients λ_1, λ_2, and λ_3 and k, the settling time of the system is reduced.[27,29,32] Therefore, the second mentioned condition related to the existence of a periodic cycle is also established with the stable control law given by Eq. (28). An important point about this control method is its dynamic structure. It should be noted that, by integrating $\dot{U}$, the bad switching effect of sign function, which produces the chattering vibration, is filtered, while its disturbance rejection ability is preserved. While after applying the control law (Eq. (28)), the negative definiteness of the derivation of Lyapunov function (Eq. (28)) is established in accordance with relation (30), the condition that the control rule given in relation Eq. (28) in reality does not lead to the saturation of control operators (because of the effect of the internal instability of the control dynamics) should be checked. To check it, we assume that the closed loop dynamics is reached to the sliding surface and the constraints are satisfied. Now it should be checked whether the remaining dynamics for U leads to a bounded response for U. To do this, the zero dynamics of the control law is rewritten by setting the constraints and the sliding surface to zero,

$$\frac{d}{dt}\left(L_f^2C(z)+L_gL_fC(z)U\right)=0\rightarrow L_f^2C(z)+L_gL_fC(z)U=const\tag{31}$$

From Eq. (31) and considering that under these conditions, the dynamics is on the sliding surface ($S=0$), and also using Eq. (22), the following equation is obtained,

$$const=0\rightarrow U=-L_gL_fC(z)^{-1}L_f^2C(z)\tag{32}$$

This shows that the control law is bounded in the steady-state response, after satisfaction of constraints. Another point is the boundedness of the control law in the transient conditions which cannot be concluded from Eq. (32), since the dynamics of the closed loop system and the dynamics of the controller are coupled to each other. However, numerical simulations show that we always have a bounded control signals.

Now, the Poincaré map is used to study about the stability of periodic cycle of locomotion and in consequence, the stability of the robot's movement. For this purpose, as mentioned, the Poincaré map is produced based on the impact event in the state space. It is to be noted that the robot should have a sufficient energy for a stable and periodic motion regarding its initial conditions. If this initial energy is less than a permissible limit, the robot is unable to reach the desired paths and the moments generated by the robot's actuators will not be able to pass the robot through instability situation and place it in the desired paths. Also, if this initial energy is greater than permissible values for producing the limit cycle, before the controller causes the robot to move in the desired paths, it moves in other paths. So the robot may fall on the ground.[7,24] By solving the equation of the SSP of the system for each initial condition, one impact point in state space (z^-) is obtained. And by using the impact

https://doi.org/10.1017/S0263574719001796 Published online by Cambridge University Press

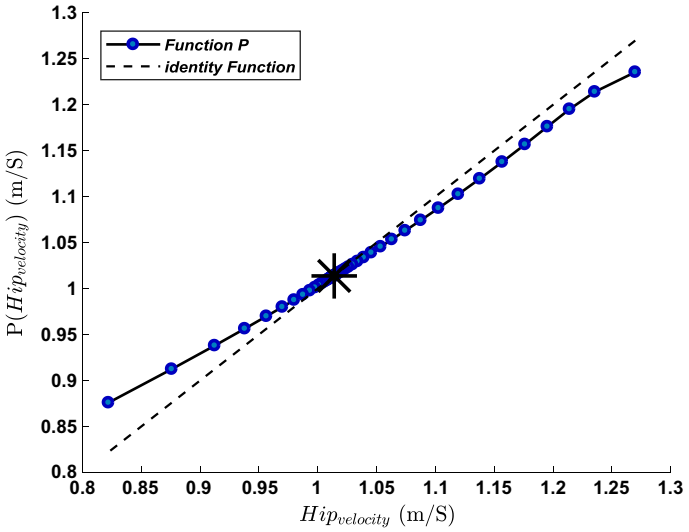


Fig. 4. Intersection between the Poincaré map P and the identity line to obtain the fixed point and the local slope of the Poincaré map; the fixed point denoted by a capital cross.

mapping function in (2), a new initial condition is formed for the dynamical system of the robot for the next SSP. By repeating this process for each new initial condition, the other impact points are obtained. As a result, a set of impact points is obtained. Therefore, the discrete function (33) is defined based on the considered Poincaré section line for the obtained impact points.

$$z_{K+1} = P(z_K) \tag{33}$$

where z_K is the vector of the system state variables at the moment of Kth impact. P is the mapping that connects these points to the next points. When the system enters the rhythmic movement, the magnitude of this vector does not change. The fixed point of this mapping, denoted by z^*, demonstrates whether the robot has a stable movement or not. This point satisfies the following equation;

$$z^* = P\left(z^*\right) \tag{34}$$

It is to be noted that the fixed point should be placed in the set of $I \cap J$. If the equilibrium point (z^*) has any kind of stability or instability, the periodic cycle has the same type of stability or instability.[2,7,23] Using the Jacobian matrix of P on z^*, one can check the stability of z^* by calculating the eigenvalues.[33,34] To have a stable periodic cycle, it is sufficient that the magnitudes of eigenvalues of the linearized map P at the fixed point are smaller than one.[1,33,35,36] To illustrate this condition, numerical calculation is used via the Taylor expansion method,

$$z^* + \Delta z_{i+1} = P\left(z^* + \Delta z_i\right) \tag{35}$$

We have,

$$z^* + \Delta z_{i+1} = P\left(z^*\right) + \left.\frac{\partial P}{\partial z}\right|_{z=z^*} \Delta z_i \tag{36}$$

where $\left.\frac{\partial P}{\partial z}\right|_{z=z^*}$ is the Jacobian matrix of P. Using the concept of hybrid zero dynamics, the dimension of the Poincaré map can be reduced to one by applying the stabilized constraints, and the horizontal velocity of the hip just before impact is selected as the states of internal dynamics to be utilized in constructing the Poincaré map.[7] In our problem, after determining the equilibrium point by numerical method as it is seen in Fig. 4, the gradient of the points in the Poincaré map (P) near the fixed point is positive and less than one. It indicates the stability of the fixed point, thus we can obtain the stable periodic cycle. For the considered values of the robot's model and constraints, the value of the horizontal hip velocity of the robot before the impact is 1.014 (m/s).

Another control method used to be compared with the FLBS control is the simple sliding mode. In ref. [37], the authors show the superiority of the sliding mode control in comparison with both

https://doi.org/10.1017/S0263574719001796 Published online by Cambridge University Press

the proportional–derivative control and the feedback linearization control. In this method, the stable surface (37) is defined like,[11]

$$S = \dot{y} + \lambda y,\ \lambda > 0 \tag{37}$$

To stabilize this control method, a reaching condition is usually utilized, which is defined as,[10,11,32,38]

$$S\dot{S} \leq -\eta S \text{sign}\,(S)\,, \quad \eta > 0 \tag{38}$$

By simplifying Eq. (38) we have,

$$\dot{S} \leq -\eta \text{sign}\,(S) \tag{39}$$

Replacing Eq. (7) into Eq. (39) yields,

$$\ddot{C}(z) + \lambda \dot{C}(z) \leq -\eta \text{sign}\,(S) \tag{40}$$

Rewriting Eq. (40) with the main variable of error dynamics (Eq. (8)) results in,

$$\left(L_f^2 C(z) + L_g L_f C(z) U\right) + \lambda L_f C(z) \leq -\eta \text{sign}\,(S) \tag{41}$$

From Eq. (41), the controller is defined as,

$$U := -L_g L_f C(z)^{-1} \left(\lambda L_f C(z) + L_f^2 C(z) + k \text{sign}\,(S)\right) \tag{42}$$

where $k \geq \eta$. Using the above mentioned control, the states reach to the sliding surface in a finite time. After that, the states converge to zero by sliding on this surface. It means that the constraints are satisfied asymptotically. In addition, because of using the sign function, the chattering occurred in the controlled system. To diminish the effect of chattering, one can use the saturation function instead of sign function which is defined as.[10]

$$\text{sat}(S, \varphi) = \begin{cases} S/\varphi & \text{if } |S| < \varphi \\ \text{sign}\,(S) & \text{other} \end{cases} \tag{43}$$

where φ determines the thickness of the boundary layer. If the boundary layer thickness increases, the control ability to converge the constraints to zero decreases and the possibility of the instability in the robot movement increases. Consequently, it is necessary to design a control method like the FLBS which can completely eliminate the adverse effects of the chattering phenomenon and stabilize the robot movement.

4. Simulations and Discussions

Two control methods described in previous section are designed and applied to the five-link underactuated biped robot and also the simulations are carried out. For simulating, it is considered an arbitrary initial condition in which the robot has enough energy for a periodic movement. Then the simulation results of both control methods are presented in presence of external disturbances on the robot dynamics to investigate the robustness of control system. By comparing the outcomes of the simulations, the following conclusions can be achieved.

It can be seen that the FLBS control method is more robust than the other control method (sliding mode control) with a less convergence time and magnitude in control signals to stabilize the system. The FLBS control can cope with higher external disturbances comparing to the sliding mode control.

The parameter of constrains on the movement mentioned in Section 2.3 is as following. The step size is 0.35 m, the desire angle of trunk is $-\pi/30$, hip joint has a sagittal path with maximum height of 0.79 m, and minimum height of 0.76 m, and the end point the of swing leg has a sagittal path with maximum height of 0.03 m. Table I presents the values of the model parameters such as length, mass, moment of inertia of each link, and the location of mass center (as shown in Fig. 1). Table II shows the parameters of two control methods.

https://doi.org/10.1017/S0263574719001796 Published online by Cambridge University Press

Table I. The robot model parameters (RABBIT robot).[2]

Values	The robot parameters	Values	The robot parameters	Values	The robot parameters
0.4(m)	L_{41}	0.2 kg.m^2	I_{41}	3.2 kg	M_{41}
0.4(m)	L_{42}	0.2 kg.m^2	I_{42}	3.2 kg	M_{42}
0.4(m)	L_{31}	0.47 kg.m^2	I_{31}	6.8 kg	M_{31}
0.4(m)	L_{32}	0.47 kg.m^2	I_{32}	6.8 kg	M_{32}
0.63(m)	L_1	1.33 kg.m^2	I_1	12 kg	M_1
0.11(m)	Z_{31}	0.24 m	Z_{42}	0.24 m	Z_{41}
		0.24 m	Z_1	0.11 m.	Z_{32}

Table II. The parameters of each control methods.

Control method	Parameter
Sliding mode for disturbance	$\lambda = [6.25, 15.625, 15.625, 6.25]$ $k = [10, 15, 15, 10]$ $\phi = 0.005$
FLBS for disturbance	$\lambda_1 = [90, 90, 90, 90]$ $\lambda_2 = [14.4, 14.4, 14.4, 14.4]$ $\lambda_3 = [14.4, 14.4, 14.4, 14.4]$ $k = [1.2, 1.2, 1.2, 1.2]$
FLBS for uncertainty	$\lambda_1 = [72, 72, 72, 72]$ $\lambda_2 = [16, 16, 16, 16]$ $\lambda_3 = [16, 16, 16, 16]$ $k = [1.1, 1.1, 1.1, 1.1]$

Table III. The magnitude of the disturbances which the control can cope with and the average value of each control signals in the stable periodic movement of the robot.

Control method	The values of disturbances (N.m)	The average magnitudes of controller's signals (N.m)
FLBS	$\begin{bmatrix} 70 \\ 70 \\ 70 \\ 70 \end{bmatrix}$	$\begin{bmatrix} 18.88 \\ 14.04 \\ 12.48 \\ 3.74 \end{bmatrix}$
Sliding mode	$\begin{bmatrix} 8 \\ 8 \\ 8 \\ 8 \end{bmatrix}$	$\begin{bmatrix} 17.02 \\ 15.9 \\ 12.99 \\ 3.9 \end{bmatrix}$

4.1. External disturbances

In the stabilization process, external disturbances are applied as torques to all joints in order to show the robustness of the control methods (of course, it can apply the disturbance to one of the joints such as hip joint; like what was done in refs. [10, 11], but here the disturbances are applied with the same values to all joints).

In simulations, the disturbances have duration of about 0.1 s (about 20% of the time period in the walking cycle) and are applied between 0.1s and 0.2 s in the time period of locomotion and are implemented in five cycles from fifth to ninth steps for five-link underactuated biped robot. Table III shows the average magnitudes of the control signals during a stable periodic cycle of locomotion for each joint. Also the maximum values of disturbances which the control can cope with are computed. For this goal, we assume that the values of control signals cannot be more than 100 (N.m), that is, the controller is tuned such that its amplitude is less than 100 (N.m) as utilized in ref. [2].

https://doi.org/10.1017/S0263574719001796 Published online by Cambridge University Press

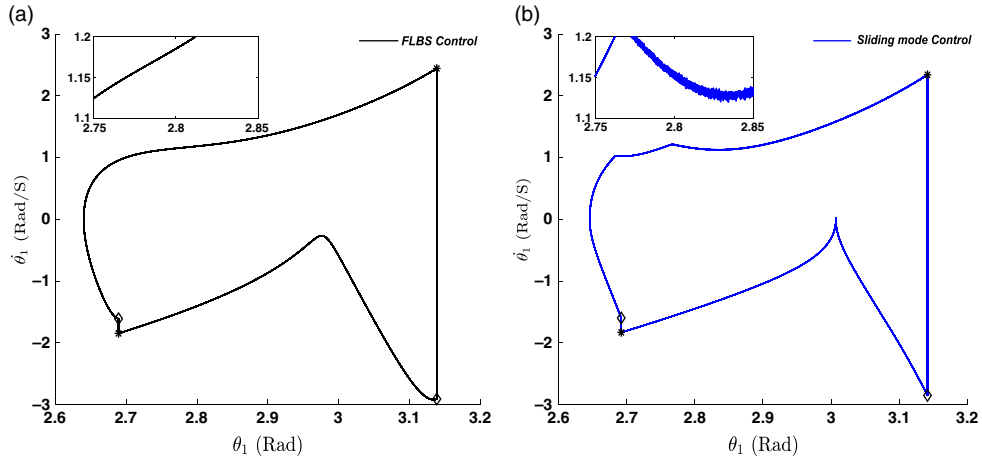


Fig. 5. Closed periodic cycles of the stance leg angle trajectory versus its velocity; the diamond sign indicates the initial condition of each SSP which turns into to a star sign at the end of DSP. (a) FLBS control method and (b) sliding mode control method.

As can be seen, the disturbances which can be applied to the system for the FLBS control method are about nine times larger than the simple sliding mode control. Generally from Table III, it is observed that the FLBS control method has the ability to stabilize the system with several times higher external disturbances in comparison to another method; besides, the average magnitude of control signals of the FLBS is less than the average magnitude of control signals of the sliding mode method in each walking cycle. In other words, the FLBS control method is more robust in comparison with another method since it can stabilize the system in the presence of more disturbance values. Because of the steady and rhythmic nature of the movement, the trajectory of the joint angles versus their velocities will be closed and repeated at every step. For example, in Fig. 5(a) and (b), the closed trajectory of the stance leg angle versus its velocity during each step is shown. The difference between Fig. 5(a) and (b) is that the sliding control method shows a chattering phenomenon in the stabilized cycles due to the existence of sign function in the control signal. This issue is strongly deduced from figures of actuator signals. The effect of chattering phenomenon can be reduced by using the saturation function, which results in some steady-state errors. But the FLBS control method showed its superiority due to the complete elimination of this phenomenon and the presence of a smoother track.

Figure 6 illustrates the time histories of control signals. The rectangular frames shown in the figure is related to the time that disturbances are applied to the system. The chattering of sliding mode control which is marked via the circular frame can be seen; however, the control signals are smooth and without chattering in the FLBS control method. Even though the absolute values of control signal in the FLBS method is more than sliding mode method when disturbances are applied, it should be noted that the disturbance values acting on this time for the FLBS method is 70 (N.m) which is about 9 times larger than those acting on the sliding mode method.

Figure 7 shows the convergence of constraints to zero. As can be seen, the constraints are satisfied before the impact occurs. From the first and the last constraint convergence, it is obtained that the FLBS method can rapidly stabilize the movement of robot and lead robot in the rhythmic motion, even though the disturbances have larger amounts.

4.2. Uncertainties in parameters

In the stabilization process, the uncertainty to the system parameters is applied in order to show the other type of robustness for the FLBS control method. For this goal, it is assumed that all parameters of mass and moment of inertia of each link have uncertainties. Simulation results are obtained for 15% uncertainty in the values of these parameters, while the maximum absolute values of control signals do not exceed 100 (N.m). The sliding mode method can stabilize the robot movement with a little larger value (104.7 (N.m)) than 100 (N.m) in control signal amounts, while this limit has not been violated by the FLBS method (see Table IV). It should be noted that, by trial and error, finally the control parameters of each method is found, which can stabilize the robot motion while

https://doi.org/10.1017/S0263574719001796 Published online by Cambridge University Press

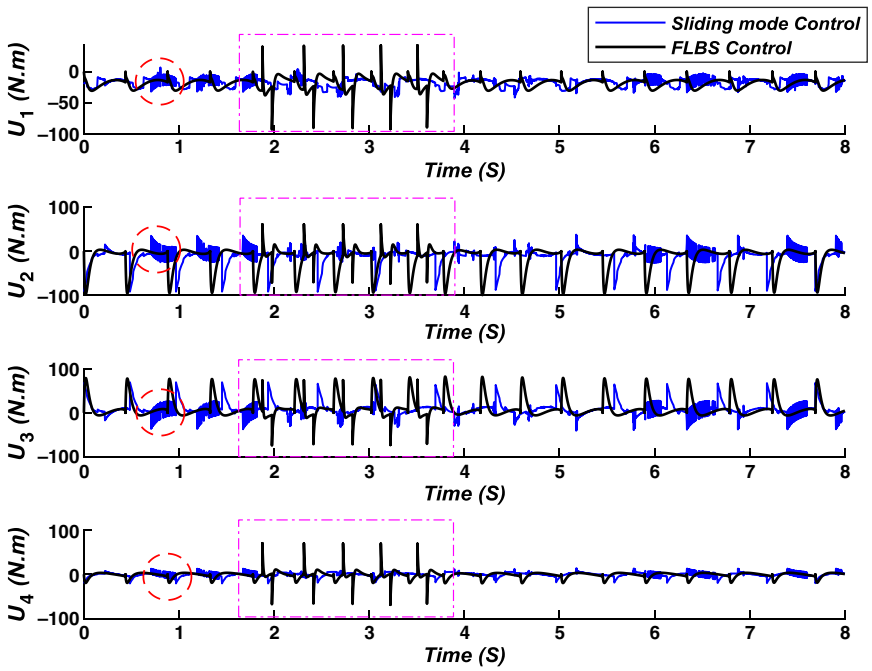


Fig. 6. Controller signals in the presence of disturbances.

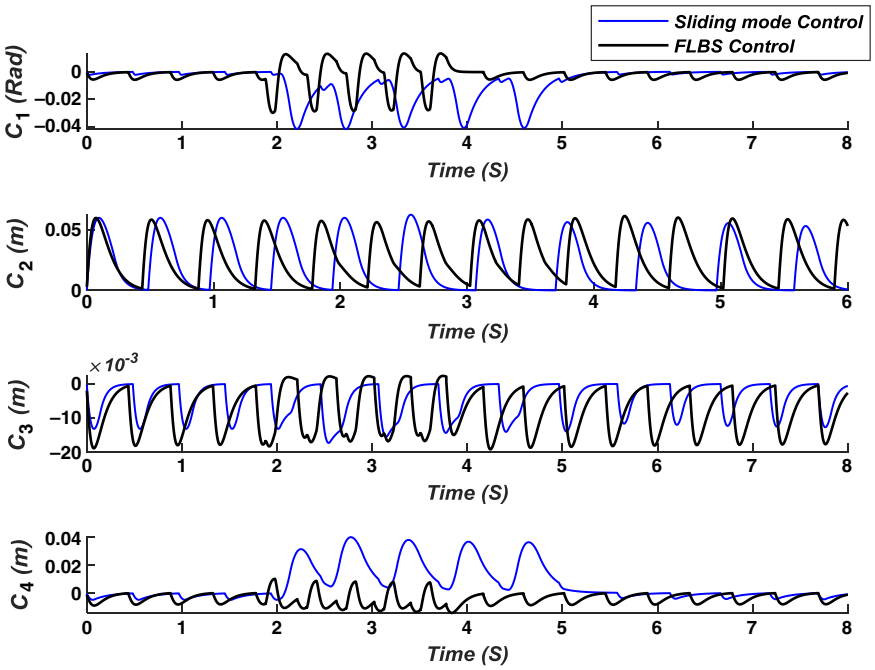


Fig. 7. Trajectories of how constraints are satisfied in the presence of disturbances.

the control signals do not exceed 100 (N.m) (though the controller in the sliding mode method has a bit larger value (104.7 (N.m)) rather than limits. It means that by a little decrement in the value of control parameters to reduce the control signal amounts, instability results. Also to stabilize the robot motion with more uncertainties, the control parameters should be increased; and so the control signals exceed 100 (N.m). Table IV represents the average, the maximum absolute (Max Abs), and the power of control signals for each method; in the first case, the mentioned parameters have +15% uncertainties in their values (i.e., the estimated values are 15% greater than the real values) and in the

https://doi.org/10.1017/S0263574719001796 Published online by Cambridge University Press

Table IV. The average values of controller signals in two cases: (a) the mentioned parameters have −15% uncertainties (b) the mentioned parameters have +15% uncertainties.

Method	**Uncertainties**	**Control signals (N.m)** [**Average**, **Max Abs**]	**Power (Watt)** [$T\omega$]
Sliding mode	Case (a) −15%	$\begin{bmatrix} -18.84, & 38.23 \\ -8.44, & 79.62 \\ 7.10, & 60.13 \\ -0.53, & 16.99 \end{bmatrix}$	$\begin{bmatrix} 15903 \\ 11204 \\ 9032 \\ 3260 \end{bmatrix}$
FLBS		$\begin{bmatrix} -15.75, & 33.08 \\ -17.46, & 99.21 \\ 14.92, & 84.51 \\ -3.31, & 20.22 \end{bmatrix}$	$\begin{bmatrix} 2132 \\ 1735 \\ 1841 \\ 640 \end{bmatrix}$
Sliding mode	Case (b) +15%	$\begin{bmatrix} -15.68, & 36.39 \\ -8.15, & 104.5 \\ 6.34, & 77.89 \\ -0.18, & 22.05 \end{bmatrix}$	$\begin{bmatrix} 20944 \\ 20101 \\ 15048 \\ 4485 \end{bmatrix}$
FLBS		$\begin{bmatrix} -12.63, & 29.59 \\ -15.47, & 99.38 \\ 11.92, & 78.15 \\ -2.16, & 19.56 \end{bmatrix}$	$\begin{bmatrix} 2074 \\ 1887 \\ 1557 \\ 800 \end{bmatrix}$

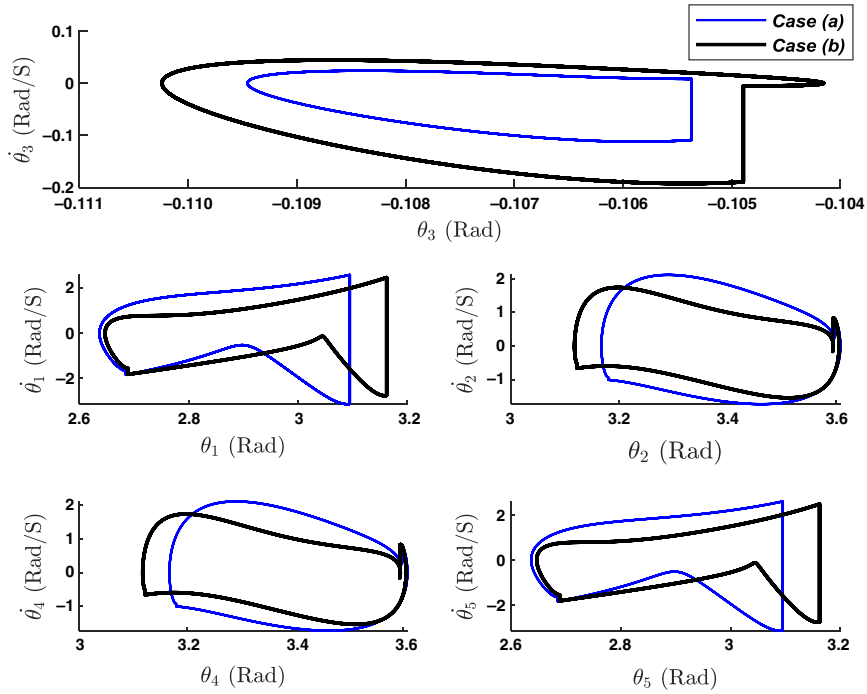


Fig. 8. Closed periodic cycles in the FLBS control method with uncertainty parameters.

second case they have −15% uncertainties in their values (i.e., the utilized values are 15% smaller than the real values).

From Table IV, it is found that in presence of 15% parameter uncertainty, the maximum absolute value of the control signal in the sliding mode method is more than the FLBS method. While the average value of control signals in the FLBS method is sometimes more than sliding mode method,

https://doi.org/10.1017/S0263574719001796 Published online by Cambridge University Press

the power consumption of controller actions in the FLBS is less. In addition, the FLBS has other advantages such as chatter-free and smooth signals comparing to the sliding mode method which has been mentioned before.

Figure 8 shows the closed cycle of link angle trajectories versus their velocities in cases (a) and (b), therefore the motion is stable. It seems that case (a), comparing to case (b), has less variation in the angles, but it has more deviation in velocities.

5. Conclusion

In this research, we proposed a new robust controller that provides a stable movement for a biped robot in the presence of external disturbances and uncertainties. The novelty of the proposed work is that the robust control law is based on the contribution of feedback linearizing, backstepping, and sliding mode methods, and this control method provides less power and chatter-free control signals. Convergence of the controlled system was ensured by a Lyapunov stability theorem. In addition, using a Poincaré map, the stable movement of the biped robot was proven. In addition to the FLBS, a standard sliding mode control method was designed to compare the performance of the two control methods with each other. With the help of some numerical simulations, it was validated that the FLBS control method has a proper performance and it is robust in the presence of external disturbances and uncertainties. The simulation results also revealed the superiority of this controller in comparison with the previously established controls based on the sliding mode.

References

1. P.-B. Wieber, R. Tedrake and S. Kuindersma, "Modeling and Control of Legged Robots," In: *Springer Handbook of Robotics*, (Springer International Publishing, Cham, 2016) pp. 1203–1234.
2. E. R. Westervelt, J. W. Grizzle, C. Chevallereau, J. H. Choi and B. Morris, "Feedback Control of Dynamic Bipedal Robot Locomotion," vol. **28**. (CRC Press, Taylor and Francis Group, New York, 2007).
3. C. Chevallereau and Y. Aoustin, "Optimal reference trajectories for walking and running of a biped robot," *Robotica.* **19**, 557–569 (2001).
4. C. Chevallereau, Y. Aoustin and A. Formal'sky, "Optimal Walking Trajectories for a Biped," Proceedings of the First Workshop on Robot Motion and Control, RoMoCo 1999 (1999) pp. 171–176.
5. J. W. Grizzle, G. Abba and F. Plestan, "Asymptotically stable walking for biped robots: Analysis via systems with impulse effects," *IEEE Trans. Autom. Cont.* **46**, 51–64 (2001).
6. J. W. Grizzle, F. Plestan and G. Abba, "Poincare's Method for Systems with Impulse Effects: Application to Mechanical Biped Locomotion," Proceedings of the 38th IEEE Conference on Decision and Control (1999) pp. 3869–3876.
7. F. Plestan, J. W. Grizzle, E. R. Westervelt and G. Abba, "Stable walking of a 7-DOF biped robot," *IEEE Trans. Robot. Autom.* **19**, 653–668 (2003).
8. S. Tzafestas, M. Raibert and C. Tzafestas, "Robust sliding-mode control applied to a 5-link biped robot," *J. Intell. Robot. Syst.* **15**, 67–133 (1996).
9. S. H. Lee, J. B. Park and Y. H. Choi, "Sliding Mode Control Based on Self-Recurrent Wavelet Neural Network for Five-Link Biped Robot," International Joint Conference *on SICE-ICASE 2006* (2006) pp. 726–731.
10. S. A. A. Moosavian, A. Takhmar and M. Alghooneh, "Regulated Sliding Mode Control of a Biped Robot," International Conference on Mechatronics and Automation, ICMA 2007 (2007) pp. 1547–1552.
11. M. Nikkhah, H. Ashrafiuon and F. Fahimi, "Robust control of underactuated bipeds using sliding modes," *Robotica.* **25**, 367–374 (2007).
12. H. B. Oza, Y. V. Orlov, S. K. Spurgeon, Y. Aoustin and C. Chevallereau, "Continuous second order sliding mode based robust finite time tracking of a fully actuated biped robot," 2014 European Control Conference (ECC) (2014), pp. 2600–2605.
13. J. Oviedo-Barriga, L. González-Jiménez, B. Castillo-Toledo and E. Bayro-Corrochano, "Robust tracking of bio-inspired references for a biped robot using geometric algebra and sliding mode control," *Robotica.* **33**, 209–224 (2015).
14. M. P. Aghababa and M. E. Akbari, "A chattering-free robust adaptive sliding mode controller for synchronization of two different chaotic systems with unknown uncertainties and external disturbances," *Appl. Math. Comput.* **218**, 5757–5768 (2012).
15. H. Li, X. Liao, C. Li and C. Li, "Chaos control and synchronization via a novel chatter free sliding mode control strategy," *Neurocomputing,* **74**, 3212–3222 (2011).
16. M. Li, Y. Hu, W. Feng, C. Wang and X. Wu, "Adaptive Sliding Mode Control for Biped Robots with sEMG Signals," 2018 IEEE International Conference on Cyborg and Bionic Systems (CBS) (2018) pp. 656–661.
17. M. Rahmani, A. Ghanbari and M. M. Ettefagh, "A novel adaptive neural network integral sliding-mode control of a biped robot using bat algorithm," *J. Vib. Control.* **24**, 2045–2060 (2018).
18. R. Heydari and M. Farrokhi, "Robust model predictive control of biped robots with adaptive on-line gait generation," *Int. J. Control, Autom. Syst.* **15**, 329–344 (2017).

https://doi.org/10.1017/S0263574719001796 Published online by Cambridge University Press

19. Q. Nguyen and K. Sreenath, "Optimal Robust Control for Bipedal Robots through Control Lyapunov Function based Quadratic Programs," Conference: Robotics: Science and Systems 2015. DOI: 10.15607/RSS.2015.XI.048.
20. V. Janardhan and R. P. Kumar, "Online trajectory generation for wide ditch crossing of biped robots using control constraints," *Robot. Auton. Syst.* **97**, 61–82 (2017).
21. C. Chevallereau, G. Bessonnet, G. Abba and Y. Aoustin, Bipedal Robots: Modeling, Design and Walking Synthesis (John Wiley & Sons, Inc., Hoboken, NJ, 2013).
22. M. M. Kakaei and H. Salarieh, "A Novel robust control method for three-link underactuated planar biped robot," *Modares Mech. Eng.* **17**, 47–58 (2017).
23. B. Morris and J. W. Grizzle, "A Restricted Poincaré Map for Determining Exponentially Stable Periodic Orbits in Systems with Impulse Effects: Application to Bipedal Robots," 44th IEEE Conference on Decision and Control, 2005 and 2005 European Control Conference. CDC-ECC 2005 (2005) pp. 4199–4206.
24. B. Morris and J. W. Grizzle, "Hybrid invariant manifolds in systems with impulse effects with application to periodic locomotion in bipedal robots," *IEEE Trans. Autom. Control,* **54**, 1751–1764 (2009).
25. E. R. Westervelt, J. W. Grizzle and C. C. De Wit, "Switching and PI control of walking motions of planar biped walkers," *IEEE Trans. Autom. Control,* **48**, 308–312 (2003).
26. T. Wang and C. Chevallereau, "Stability analysis and time-varying walking control for an under-actuated planar biped robot," *Robot. Auton. Syst.* **59**, 444–456 (2011).
27. H. K. Khalil, Noninear Systems, vol. 2, p. 5.1, (Prentice-Hall, New Jersey, 1996).
28. S. K. Y. Nikravesh, *Nonlinear Systems Stability Analysis: Lyapunov-Based Approach* (CRC Press, 2013).
29. M. Vidyasagar, *Nonlinear Systems Analysis* (SIAM, 2002).
30. A. Isidori, *Nonlinear Control Systems, An Introduction* (Springer-Verlag, Berlin, Heidelberg, 1989).
31. M. W. Spong and M. Vidyasagar, *Robot Dynamics and Control* (John Wiley & Sons, Wiley India Pvt. Limited, 2008).
32. W. Perruquetti and J.-P. Barbot, *Sliding Mode Control in Engineering* (CRC Press, Taylor and Francis Group, Boca Raton, 2002).
33. S. Gupta and A. Kumar, "A brief review of dynamics and control of underactuated biped ," Adv. Robot. **31**(12), 1–17 (2017).
34. R. W. Sinnet and A. D. Ames, "2D Bipedal Walking with Knees and Feet: A Hybrid Control Approach," Proceedings of the 48th IEEE Conference on Decision and Control, 2009 held jointly with the 2009 28th Chinese Control Conference. CDC/CCC 2009 (2009) pp. 3200–3207.
35. Y. M. R. Hairi, M. R. Sabaapour and B. Beigzadeh, "Asymptotically Stable Walking Control of a 3D Biped Robot Via Potential Energy Shaping Approach," *Modares Mech. Eng*. **15**, 261–270 (2015).
36. M. Yosofvand, B. Beigzadeh and M. A. H. Davaie, "Analysis of stable period-one gait of a planner passive biped with elasti links," *Modares Mech. Eng*. **16**, 312–320 (2016).
37. M. Raibert, S. Tzafestas and C. Tzafestas, "Comparative Simulation Study of Three Control Techniques Applied to a Biped Robot," *Proceedings of the International Conference on* 'Systems Engineering in the Service of Humans', Conference *Systems, Man and Cybernetics* (1993) pp. 494–502.
38. M. Taherkhorsandi, M. Mahmoodabadi, M. Talebipour and K. Castillo-Villar, "Pareto design of an adaptive robust hybrid of PID and sliding control for a biped robot via genetic algorithm optimization," *Nonlin. Dynam.* **79**, 251–263 (2015).

https://doi.org/10.1017/S0263574719001796 Published online by Cambridge University Press